

A photonic which-path entangler based on longitudinal cavity-qubit coupling

Z. M. McIntyre* and W. A. Coish†

Department of Physics, McGill University, 3600 rue University, Montreal, QC, H3A 2T8, Canada

(Dated: January 31, 2024)

We show that a modulated longitudinal cavity-qubit coupling can be used to control the path taken by a multiphoton coherent-state wavepacket conditioned on the state of a qubit, resulting in a qubit-which-path (QWP) entangled state. QWP states can generate long-range multipartite entanglement using strategies for interfacing discrete- and continuous-variable degrees-of-freedom. Using the approach presented here, entanglement can be distributed in a quantum network without the need for single-photon sources or detectors.

Fault-tolerant quantum computing will require redundancy to identify and correct errors during a computation. In most architectures, the physical qubits will therefore vastly outnumber the logical qubits. The need to scale up existing architectures has motivated a network approach where remote qubits, grouped into nodes, are connected by quantum-photonic interconnects [1–5]. These quantum networks naturally require entanglement distribution across nodes. Consequently, significant effort has gone towards generating both heralded [6–12] and deterministic [13–20] qubit-photon entanglement.

In this Letter, we present a photonic which-path entangler that correlates the path of an incoming multiphoton coherent-state wavepacket with the state of a cavity-coupled control qubit (Fig. 1). The resulting which-path degree of freedom, consisting of a coherent-state wavepacket traveling in one of two transmission lines, can be re-encoded in the photon-number parity of a continuous-variable degree-of-freedom, then used to generate entanglement with one or more distant qubits. The entangler presented here therefore provides a natural interface between discrete- and continuous-variable approaches to hybrid quantum computation [21–26]. The qubit-which-path (QWP) state generated by the entangler also has greater potential sensitivity for phase measurements than either the comparable entangled coherent state (ECS) [27, 28] (consisting of a superposition of coherent states, one in each interferometer arm) or NOON state [29–31] (an analogous superposition of N -photon Fock states). Quantum-enhanced interferometry has applications in, e.g., biological imaging [32–34] and gravitational wave detection [35–38].

A key requirement for the entangler is a modulated longitudinal (qubit-eigenstate preserving) cavity-qubit coupling. Longitudinal coupling has attracted significant theoretical and experimental attention in recent years, as it is currently being realized and leveraged in a number of promising quantum-computing architectures [10, 39–41, 43–49]. Though many current implementations of, e.g., cavity-coupled spin, charge, and superconducting qubits make use of the (transverse) Rabi coupling, longitudinal cavity-qubit couplings are no less fundamental. They can be engineered for single-electron-spin qubits in double quantum dots (DQDs), which can be coupled to

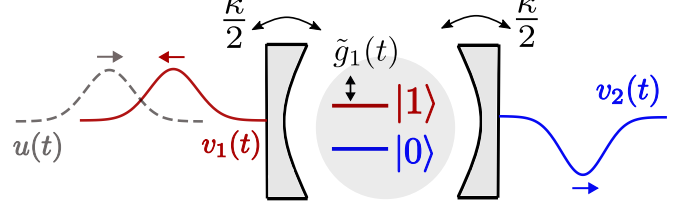


FIG. 1. In the presence of a longitudinal cavity-qubit coupling modulated at the cavity frequency with envelope $\tilde{g}_1(t)$, an incoming coherent state with waveform $u(t)$ is reflected (transmitted) into a coherent state with waveform $v_1(t)$ [$v_2(t)$] for control-qubit state $|1\rangle$ ($|0\rangle$). This effect requires symmetric decay rates $\kappa_1 = \kappa_2 = \kappa/2$ for cavity ports $i = 1, 2$.

cavity electric fields via magnetic-field gradients [10], as well as for hole-spin qubits in semiconductors [47, 49, 50], which interact with electric fields via their large intrinsic spin-orbit coupling. Two-electron-spin singlet-triplet qubits in DQDs can be longitudinally coupled to electric fields by modulating a gate voltage controlling the strength of the exchange interaction [45, 48]. Longitudinal coupling can also be engineered in various superconducting-qubit architectures [39–41, 43, 44]. Moreover, even in systems where the dominant source of cavity-qubit coupling is intrinsically transverse, an effectively longitudinal interaction can be engineered (in some rotating frame) by modulating the coupling strength at both the cavity and qubit frequencies [46], making the theory presented here widely applicable.

Model—A longitudinal cavity-qubit interaction arises, e.g., from the DC Stark shift due to electric dipole coupling ($\propto Ey$ for a cavity electric field E polarized along \hat{y}). Quantizing the cavity field (focusing on a single cavity mode of frequency ω_c and annihilation operator a), and in adiabatic perturbation theory, we find an interaction proportional to the product of $E \propto i(a^\dagger - a)$ and the dipole matrix element $\langle s(t)|y|s(t)\rangle$ taken with respect to the instantaneous qubit energy eigenstate $|s(t)\rangle$ ($s = 0, 1$) [51]. This gives an effective Hamiltonian $H_{\text{eff}}(t) = \sum_s i g_s(t)(a^\dagger - a)|s\rangle\langle s|$, where $|s\rangle$ is a time-independent state in the adiabatic frame, and where $g_s(t) = g_s[\{x_j(t)\}] \propto \langle s(t)|y|s(t)\rangle$ inherits time dependence from a collection of control parameters $\{x_j\}$ that

determine $|s(t)\rangle$. For spin qubits, the spin-dependent electric dipole matrix elements [and consequently $g_s(t)$] can be modulated through external electric fields or gate voltages [10, 47, 49]. An analogous mechanism exists for flux-tunable superconducting transmon qubits, in which the couplings $g_s(t)$ can instead be tuned by modulating a flux [41]. In what follows, we assume a time-independent value $g_0(t) = \bar{g}_0$ and a sinusoidal modulation of $g_1(t)$ at the cavity frequency, $g_1(t) = \bar{g}_1 + 2|\tilde{g}_1(t)|\cos[\omega_c t - \vartheta(t)]$, where $\tilde{g}_1(t) = e^{i\vartheta(t)}|\tilde{g}_1(t)|$ is a slowly varying envelope with $\tilde{g}_1(0) \simeq 0$ and duration τ . (See the Supplementary Material, Ref. 51, for a sufficient condition on the parameters $\{x_j\}$ in general, as well as specific conditions to achieve this coupling modulation for double-quantum-dot charge and spin qubits.) A polaron transformation can then be used to eliminate the term $\propto \bar{g}_0$ by incorporating a small shift $\sim \bar{g}_0^2/\omega_c$ in the qubit frequency ω_q . Going to an interaction picture with respect to the decoupled Hamiltonian $\omega_c a^\dagger a + \omega_q \sigma_z/2$ ($\sigma_z = |0\rangle\langle 0| - |1\rangle\langle 1|$), and within a rotating-wave approximation requiring that $|\bar{g}_1|, |\tilde{g}_1(t)| \ll \omega_c$, the cavity-qubit Hamiltonian is then given by [51]

$$H_0(t) = \frac{\xi(t)}{2} \sigma_z + i|1\rangle\langle 1| [\tilde{g}_1(t) a^\dagger - \text{h.c.}], \quad (1)$$

where we have introduced a stochastic noise parameter $\xi(t)$ leading to qubit dephasing. In general, the dipole approximation also produces a transverse Rabi term $[ig_\perp \sigma_x (a^\dagger - a)]$, which, in the regime $|g_\perp| < |\delta|$ ($\delta = \omega_q - \omega_c$), leads to a dispersive coupling $\chi \sigma_z a^\dagger a$, where $\chi = g_\perp^2/\delta$. Any effects due to transverse coupling can be suppressed by operating in the regime $|g_\perp| \ll |\delta|$.

The longitudinal interaction $\propto \tilde{g}_1(t)$ displaces the cavity vacuum into a finite-amplitude coherent state for $s = 1$. A similar effect is studied in Ref. 41 to design a fast quantum non-demolition (QND) qubit readout. Relative to Ref. 41, we additionally consider driving of the cavity by an input field. In particular, we assume that the cavity is coupled to external transmission lines at input ($i = 1$) and output ($i = 2$) ports (Fig. 1). An input spatiotemporal mode (wavepacket) with normalized waveform $u(t)$ [$\int dt |u(t)|^2 = 1$] can be represented by the mode operator $b_u = \int dt u^*(t) r_{\text{in},1}(t)$ [52, 53], where $r_{\text{in},i}(t)$ satisfies the input-output relation $r_{\text{out},i}(t) = r_{\text{in},i}(t) + \sqrt{\kappa_i} a(t)$ [54]. Here, $r_{\text{out},i}(t)$ is the output field, and κ_i is the rate of decay from cavity port i . We assume that the quantum state of the incoming wavepacket is a coherent state with initial amplitude $\langle b_u \rangle = \alpha_0$, giving $\langle r_{\text{in},1} \rangle_t = u(t) \alpha_0$. Where it appears, the notation $\langle \mathcal{O} \rangle_t$ indicates an average with respect to the initial state $\rho(0)$: $\langle \mathcal{O} \rangle_t = \text{Tr}\{\mathcal{O}(t)\rho(0)\}$ for operator \mathcal{O} . The reflected and transmitted waveforms are given in the frequency domain by $v_1(\omega) = R(\omega)u(\omega)$ and $v_2(\omega) = T(\omega)u(\omega)$, respectively, where $R(\omega) = \langle r_{\text{out},1} \rangle_\omega / \langle r_{\text{in},1} \rangle_\omega$ and $T(\omega) = \langle r_{\text{out},2} \rangle_\omega / \langle r_{\text{in},1} \rangle_\omega = \sqrt{\kappa_2} \langle a \rangle_\omega / \alpha_0 u(\omega)$ are the reflection and transmission coefficients with $\langle \mathcal{O} \rangle_\omega = \int dt e^{i\omega t} \langle \mathcal{O} \rangle_t$.

To derive the transmission $T(\omega)$ conditioned on the qubit state $|s\rangle$, we now find $\langle a \rangle_\omega$ from the quantum Langevin equation for $\langle a \rangle_t$,

$$\langle \dot{a} \rangle_t = -\frac{\kappa}{2} \langle a \rangle_t + \tilde{g}_1(t)s - \sqrt{\kappa_1} \alpha_0 u(t). \quad (2)$$

The displacement of the cavity vacuum due to the interaction $\propto \tilde{g}_1(t)$ can therefore be canceled exactly, conditioned on the qubit being in state $|1\rangle$, by ensuring that $\sqrt{\kappa_1} \alpha_0 u(t) = \tilde{g}_1(t)$. Destructive interference then precludes a transfer of photons to the output transmission line, leading to perfect reflection of the input field. Evidence of such destructive interference was recently observed experimentally in Ref. 55, where a modulated longitudinal coupling and a cavity drive were both generated with a common voltage source (acting as a common phase reference). Because the input state is a coherent state [and coherent states are eigenstates of $r_{\text{in},1}(t)$], there are no quantum fluctuations about the average dynamics $\langle r_{\text{in},1} \rangle_t = \alpha_0 u(t)$. For a non-ideal input, however, fluctuations about the average ($\alpha_0 \rightarrow \alpha_0 + \delta\alpha$) lead to imperfect cancellation for $s = 1$.

For a cavity that is initially empty, we have $\langle a \rangle_0 = 0$. Integrating the quantum Langevin equation [Eq. (2)] with this initial condition gives

$$\langle a \rangle_\omega = \chi_c(\omega) [\tilde{g}_1(\omega)s - \sqrt{\kappa_1} \alpha_0 u(\omega)], \quad (3)$$

where $\chi_c(\omega) = (\kappa/2 - i\omega)^{-1}$. For $\sqrt{\kappa_1} \alpha_0 u(\omega) = \tilde{g}_1(\omega)$, the transmission can then be written as

$$T(\omega) = (1 - s) \frac{\sqrt{\kappa_1 \kappa_2}}{i\omega - \kappa/2}. \quad (4)$$

The input pulse $u(\omega)$ has support for $\omega \lesssim 1/\tau$ localized about the cavity frequency (corresponding to $\omega = 0$ in the rotating frame). Near-perfect transmission can then be achieved for $s = 0$ and $\kappa_1 = \kappa_2 = \kappa/2$ by operating in the regime of large $\kappa\tau$, where $\chi_c(\omega)$ is much broader in frequency than $u(\omega)$. Finite-bandwidth effects for a Gaussian input waveform $u(t)$ may be neglected provided [51] $N = |\alpha_0|^2 \ll (\kappa\tau)^4$. Given $T(\omega)$ for a fixed value of s , $R(\omega)$ is related to $T(\omega)$ through the input-output relation, $\sqrt{\kappa_2}[R(\omega) - 1] = \sqrt{\kappa_1}T(\omega)$.

An alternative way to condition the cavity transmission on the state of a qubit would be to engineer a qubit-state-dependent shift of the cavity frequency using dispersive coupling $\chi \sigma_z a^\dagger a$, where $2|\chi| \gg \kappa$. A narrow-band input tone at frequency χ would then be transmitted conditioned on state $|0\rangle$ and reflected for state $|1\rangle$. However, in the dispersive regime ($\epsilon = |g_\perp|/\delta < 1$), this necessarily requires (very) strong coupling $|g_\perp| \gg \kappa/\epsilon$. The entangler presented here, by contrast, can be operated even if $|\tilde{g}_1| \lesssim \kappa$. Dipole-induced transparency [56] and reflection [57] also result in perfect steady-state transmission or reflection of a weak input pulse conditional on the presence of a resonant, transversally coupled dipole. These effects are not, however, QND in the

state of the decoupled dipole and furthermore require that the cavity be driven with an average of $N_{\text{cav}} \lesssim 1$ intracavity photon [58]. For the entangler presented here, by contrast, the transmission vs reflection of a transient pulse is QND; it is conditioned on the decoupled qubit state $|s\rangle$. Moreover, the entangler works in the regime $N_{\text{cav}} \sim N/(\kappa\tau) > 1$, provided the finite-bandwidth condition is satisfied [$N \ll (\kappa\tau)^4$ for a Gaussian waveform].

The qubit-state-conditioned transmission [Eq. (4)] can be used to generate entangled states. To describe the states associated with the reflected and transmitted fields, we use the virtual-cavity formalism of Refs. [52, 53] to recast the input, reflected, and transmitted wavepackets as the fields emitted from—or absorbed into—fictitious (virtual) single-sided cavities coupled to the transmission lines via time-dependent couplings. This formalism allows for an efficient description of the scattering of an input pulse into pre-specified spatiotemporal modes, which can be modeled as the modes of virtual cavities. Accounting for the input pulse, cavity field, reflected pulse, and transmitted pulse, the evolution of the cavity and transmission lines is then fully described by an effective four-mode model. The quantum master equation governing this evolution is [52, 53]

$$\dot{\rho}_\xi = -i[H_0(t) + V(t), \rho_\xi] + \sum_{i=1,2} \mathcal{D}[L_i]\rho_\xi, \quad (5)$$

where ρ_ξ is the density matrix conditioned on a realization of the noise $\xi(t)$, and where

$$V(t) = \frac{i}{2}[\sqrt{\kappa_1}\lambda_u^*(t)a_u^\dagger a + \sum_{i=1,2} \sqrt{\kappa_i}\lambda_{v_i}(t)a^\dagger a_{v_i} + \lambda_u^*(t)\lambda_{v_1}(t)a_u^\dagger a_{v_1} - \text{h.c.}]. \quad (6)$$

In Eq. (5), $\mathcal{D}[L]\rho = L\rho L^\dagger - \frac{1}{2}\{L^\dagger L, \rho\}$ is a damping superoperator. The operators $L_1 = \sum_{\mu=u,v_1} \lambda_\mu(t)a_\mu + \sqrt{\kappa_1}a$ and $L_2 = \lambda_{v_2}(t)a_{v_2} + \sqrt{\kappa_2}a$ model decay from the virtual cavity modes a_μ , as well as decay out of the cavity mode a with rate $\kappa = \kappa_1 + \kappa_2$. The couplings to the virtual cavities are given by $\lambda_u(t) = u(t)/(\int_t^\infty dt' |u(t')|^2)^{1/2}$ and $\lambda_{v_i}(t) = (-1)^i v_i(t)/(\int_0^t dt' |v_i(t')|^2)^{1/2}$ [52, 53, 59]. The i -dependent sign in λ_{v_i} reflects the fact that in our model, a transmitted pulse undergoes a π phase shift [cf Eq. (4)]. The couplings $\lambda_u(t)$ and $\lambda_{v_i}(t)$ have singularities at $t \rightarrow \infty$ and $t = 0$, respectively, and, for real cavities, both $\lambda_u(t)$ and $\lambda_{v_i}(t)$ would have to be truncated to finite values to realize absorption (emission) into (out of) a chosen spatiotemporal mode [59]. In the virtual-cavity formalism, however, these unphysical couplings are abstractions used to calculate the dynamics into/out of a chosen mode. No additional (real) cavities or time-dependent couplings are required to realize the entangler.

We assume a fast $\pi/2$ pulse can be used to prepare the qubit in the $(t = 0)$ initial state $|+\rangle = (|1\rangle + |0\rangle)/\sqrt{2}$,

with the cavity in the vacuum state ($\langle a \rangle_0 = 0$). A coherent-state wavepacket then evolves from the input mode a_u to the two output modes a_{v_i} ($i = 1, 2$). For times $t \gg \tau$ exceeding the duration of the input pulse, the quantum states associated with the reflected and transmitted waveforms $v_i(t)$, conditioned on s , will have been fully transferred into their respective fictitious cavities: $\alpha_{is} = \lim_{t \rightarrow \infty} \langle a_{v_i} \rangle_t = (-1)^{i-1} \alpha_0 \int \frac{d\omega}{2\pi} |v_i(\omega)|^2$. The joint state of the qubit and transmission lines, found from a direct integration of Eq. (5), is then $\rho(t) = \langle\langle \rho_\xi(t) \rangle\rangle$, where $\langle\langle \rangle\rangle$ denotes an average over realizations of $\xi(t)$, and where $\rho_\xi(t) = |\Psi_{\xi(t)}\rangle \langle \Psi_{\xi(t)}|$ with

$$|\Psi_{\xi(t)}\rangle = \frac{1}{\sqrt{2}} \left(e^{\frac{i}{2}\theta_\xi(t)} |1, \psi_1\rangle + e^{-\frac{i}{2}\theta_\xi(t)} |0, \psi_0\rangle \right). \quad (7)$$

Here, $\theta_\xi(t) = \int_0^t dt' \xi(t')$ is a random phase, $|\psi_s\rangle = \prod_{i=1,2} D_i(\alpha_{is}) |\text{vac}\rangle$ is the state of the transmission lines conditioned on s , $|\text{vac}\rangle$ is the vacuum, and $D_i(\alpha) = \exp\{\alpha a_{v_i}^\dagger - \text{h.c.}\}$ is a displacement operator. For $\kappa_1 = \kappa_2 = \kappa/2$ and up to corrections in $N/(\kappa\tau)^4 \ll 1$, only one of α_{is} is nonzero for each value of s : For $s = 1$, $\alpha_{11} = \alpha_0$ and $\alpha_{21} = 0$, while for $s = 0$, $\alpha_{10} = 0$ and $\alpha_{20} = -\alpha_0$. Equation (7) therefore describes a photonic which-path qubit entangled with the control qubit (a QWP state). Under the same finite-bandwidth conditions, imperfections in the input source such that $\alpha_0 \rightarrow \alpha_0 + \delta\alpha$ will lead instead to $\alpha_{11} = \alpha_0$, $\alpha_{21} = -\delta\alpha$, $\alpha_{10} = 0$, and $\alpha_{20} = -(\alpha_0 + \delta\alpha)$. This follows from integrating the Langevin equation [Eq. (2)] with $\alpha_0 \rightarrow \alpha_0 + \delta\alpha$ and solving for the reflected and transmitted fields. If we take $\delta\alpha$ to be a complex-valued, zero-mean Gaussian random variable, then the fidelity of the ideal QWP state [Eq. (7) with $\xi = 0$] with respect to the mixed state obtained by averaging over $\delta\alpha$ is $e^{-\langle |\delta\alpha|^2 \rangle_{\delta\alpha}}$, where here, $\langle \rangle_{\delta\alpha}$ describes an average over $\delta\alpha$. High-fidelity QWP states therefore require a stable coherent-state source with a low absolute noise level, below one photon per pulse ($\langle |\delta\alpha|^2 \rangle_{\delta\alpha} \ll 1$).

Entanglement distribution—The which-path degree-of-freedom can be entangled with a second (“target”) qubit for long-range entanglement distribution. Crucially, this also provides a direct avenue for quantifying entanglement in QWP states through measurements of stationary qubits only. The setup is illustrated schematically in Fig. 2. By interfering the reflected and transmitted fields at a 50:50 beamsplitter, the output modes can be mapped to new modes a_\pm such that $\langle a_{\pm,s} \rangle = (\alpha_{1s} \pm \alpha_{2s})/\sqrt{2}$. This gives $\langle a_{-,s} \rangle = \alpha$ independent of s , where $\alpha = \alpha_0/\sqrt{2}$. The a_+ mode, by contrast, has s -dependence given by $\langle a_{+,s} \rangle = (2s - 1)\alpha$. The beamsplitter consequently reencodes the which-path degree-of-freedom in the phase of the coherent-state amplitude: $\langle a_{+,1} \rangle = +\alpha$ and $\langle a_{+,0} \rangle = -\alpha$.

For clarity, we now set $\xi(t) = 0$ for the purpose of explaining the protocol. The effects of dephasing [$\xi(t) \neq 0$] are included in the relevant result, Eq. (8), below. Since

pulse duration $\tau \sim 100 \text{ ns} \ll T_2^*$ (for transmons, coherence times reach $T_2^* \simeq 100 \mu\text{s}$ [70]).

Precision metrology—The entangler described above can also be used to perform quantum-enhanced precision measurements of a phase ϕ acquired by the field reflected from the cavity as it propagates along arm 1 of an interferometer (Fig. 2). The fundamental precision bound for estimation of ϕ (the quantum Cramér-Rao bound [71, 72]) is better for QWP states than for either NOON states (superpositions of N -photon Fock states, one in each interferometer arm) or entangled coherent states [27] (similarly, superpositions of coherent states) having the same average number N of photons [73].

Outlook—The entangler presented here could also be used to perform measurements of the phase acquired by the control qubit. Specifically, a modulated longitudinal coupling, followed by a rapid reset [74–77] $|0\rangle \rightarrow |1\rangle$, can be used to map the relative phase $|0\rangle + e^{i\theta} |1\rangle$ of the initial qubit state onto the state $|- \alpha\rangle + e^{i\theta} |\alpha\rangle$ of the a_+ mode. A projective measurement of $|C_{\pm}\rangle$ then yields a single bit of information about θ (the maximum achievable for a single-shot qubit readout). This may be useful in situations where θ encodes information about dynamics induced by a classical or quantum environment [78, 79].

Acknowledgments—We thank A. Blais and K. Wang for useful discussions. We also acknowledge funding from the Natural Sciences and Engineering Research Council (NSERC) and from the Fonds de recherche–Nature et technologies (FRQNT).

* zoe.mcintyre@mail.mcgill.ca

† william.coish@mcgill.ca

- [1] T. E. Northup and R. Blatt, Quantum information transfer using photons, *Nat. Photon.* **8**, 356 (2014).
- [2] A. Reiserer and G. Rempe, Cavity-based quantum networks with single atoms and optical photons, *Rev. Mod. Phys.* **87**, 1379 (2015).
- [3] L. M. K. Vandersypen, H. Bluhm, J. S. Clarke, A. S. Dzurak, R. Ishihara, A. Morello, D. J. Reilly, L. R. Schreiber, and M. Veldhorst, Interfacing spin qubits in quantum dots and donors—hot, dense, and coherent, *Npj Quantum Inf.* **3**, 34 (2017).
- [4] D. Awschalom, K. K. Berggren, H. Bernien, S. Bhawe, L. D. Carr, P. Davids, S. E. Economou, D. Englund, A. Faraon, M. Fejer, *et al.*, Development of quantum interconnects (quics) for next-generation information technologies, *PRX Quantum* **2**, 017002 (2021).
- [5] M. Ruf, N. H. Wan, H. Choi, D. Englund, and R. Hanson, Quantum networks based on color centers in diamond, *J. Appl. Phys.* **130**, 070901 (2021).
- [6] L.-M. Duan, B. B. Blinov, D. L. Moehring, and C. Monroe, Scalable trapped ion quantum computation with a probabilistic ion-photon mapping, *Quantum Inf. Comput.* **4**, 165 (2004).
- [7] J. Hofmann, M. Krug, N. Ortegel, L. Gérard, M. Weber, W. Rosenfeld, and H. Weinfurter, Heralded entanglement between widely separated atoms, *Science* **337**, 72 (2012).
- [8] H. Bernien, B. Hensen, W. Pfaff, G. Koolstra, M. S. Blok, L. Robledo, T. H. Taminiau, M. Markham, D. J. Twitchen, L. Childress, and R. Hanson, Heralded entanglement between solid-state qubits separated by three metres, *Nature* **497**, 86 (2013).
- [9] B. Hensen, H. Bernien, A. E. Dréau, A. Reiserer, N. Kalb, M. S. Blok, J. Ruitenberg, R. F. L. Vermeulen, R. N. Schouten, C. Abellán, *et al.*, Loophole-free Bell inequality violation using electron spins separated by 1.3 kilometres, *Nature* **526**, 682 (2015).
- [10] A. Delteil, Z. Sun, W.-b. Gao, E. Togan, S. Faelt, and A. Imamoglu, Generation of heralded entanglement between distant hole spins, *Nat. Phys.* **12**, 218 (2016).
- [11] A. Narla, S. Shankar, M. Hatridge, Z. Leghtas, K. M. Sliwa, E. Zals-Geller, S. O. Mundhada, W. Pfaff, L. Frunzio, R. J. Schoelkopf, *et al.*, Robust concurrent remote entanglement between two superconducting qubits, *Phys. Rev. X* **6**, 031036 (2016).
- [12] M. Pompili, S. L. N. Hermans, S. Baier, H. K. C. Beukers, P. C. Humphreys, R. N. Schouten, R. F. L. Vermeulen, M. J. Tiggelman, L. dos Santos Martins, B. Dirkse, S. Wehner, and R. Hanson, Realization of a multinode quantum network of remote solid-state qubits, *Science* **372**, 259 (2021).
- [13] J. I. Cirac, P. Zoller, H. J. Kimble, and H. Mabuchi, Quantum state transfer and entanglement distribution among distant nodes in a quantum network, *Phys. Rev. Lett.* **78**, 3221 (1997).
- [14] S. Ritter, C. Nölleke, C. Hahn, A. Reiserer, A. Neuzner, M. Uphoff, M. Mücke, E. Figueroa, J. Bochmann, and G. Rempe, An elementary quantum network of single atoms in optical cavities, *Nature* **484**, 195 (2012).
- [15] P. Kurpiers, P. Magnard, T. Walter, B. Royer, M. Pechal, J. Heinsoo, Y. Salathé, A. Akin, S. Storz, J.-C. Besse, *et al.*, Deterministic quantum state transfer and remote entanglement using microwave photons, *Nature* **558**, 264 (2018).
- [16] C. J. Axline, L. D. Burkhardt, W. Pfaff, M. Zhang, K. Chou, P. Campagne-Ibarcq, P. Reinhold, L. Frunzio, S. M. Girvin, L. Jiang, *et al.*, On-demand quantum state transfer and entanglement between remote microwave cavity memories, *Nat. Phys.* **14**, 705 (2018).
- [17] P. Campagne-Ibarcq, E. Zals-Geller, A. Narla, S. Shankar, P. Reinhold, L. Burkhardt, C. Axline, W. Pfaff, L. Frunzio, R. J. Schoelkopf, *et al.*, Deterministic remote entanglement of superconducting circuits through microwave two-photon transitions, *Phys. Rev. Lett.* **120**, 200501 (2018).
- [18] N. Leung, Y. Lu, S. Chakram, R. K. Naik, N. Earnest, R. Ma, K. Jacobs, A. N. Cleland, and D. I. Schuster, Deterministic bidirectional communication and remote entanglement generation between superconducting qubits, *Npj Quantum Inf.* **5**, 18 (2019).
- [19] P. Magnard, S. Storz, P. Kurpiers, J. Schär, F. Marxer, J. Lütolf, T. Walter, J.-C. Besse, M. Gabureac, K. Reuer, *et al.*, Microwave quantum link between superconducting circuits housed in spatially separated cryogenic systems, *Phys. Rev. Lett.* **125**, 260502 (2020).
- [20] Y. Zhong, H.-S. Chang, A. Bienfait, É. Dumur, M.-H. Chou, C. R. Conner, J. Grebel, R. G. Povey, H. Yan, D. I. Schuster, *et al.*, Deterministic multi-qubit entanglement in a quantum network, *Nature* **590**, 571 (2021).
- [21] U. L. Andersen, J. S. Neergaard-Nielsen, P. Van Loock,

- and A. Furusawa, Hybrid discrete-and continuous-variable quantum information, *Nat. Phys.* **11**, 713 (2015).
- [22] S. Takeda, M. Fuwa, P. van Loock, and A. Furusawa, Entanglement swapping between discrete and continuous variables, *Phys. Rev. Lett.* **114**, 100501 (2015).
- [23] K. Huang, H. Le Jeannic, O. Morin, T. Darras, G. Guccione, A. Cavaillès, and J. Laurat, Engineering optical hybrid entanglement between discrete-and continuous-variable states, *New J. Phys.* **21**, 083033 (2019).
- [24] G. Guccione, T. Darras, H. Le Jeannic, V. B. Verma, S. W. Nam, A. Cavaillès, and J. Laurat, Connecting heterogeneous quantum networks by hybrid entanglement swapping, *Sci. Adv.* **6**, eaba4508 (2020).
- [25] I. B. Djordjevic, Hybrid CV-DV quantum communications and quantum networks, *IEEE Access* **10**, 23284 (2022).
- [26] T. Darras, B. E. Asenbeck, G. Guccione, A. Cavaillès, H. Le Jeannic, and J. Laurat, A quantum-bit encoding converter, *Nat. Photon.* **17**, 165 (2023).
- [27] B. C. Sanders, Entangled coherent states, *Physical Review A* **45**, 6811 (1992).
- [28] J. Joo, W. J. Munro, and T. P. Spiller, Quantum metrology with entangled coherent states, *Phys. Rev. Lett.* **107**, 083601 (2011).
- [29] J. J. Bollinger, W. M. Itano, D. J. Wineland, and D. J. Heinzen, Optimal frequency measurements with maximally correlated states, *Phys. Rev. A* **54**, R4649 (1996).
- [30] H. Lee, P. Kok, and J. P. Dowling, A quantum Rosetta stone for interferometry, *J. Mod. Opt.* **49**, 2325 (2002).
- [31] V. Giovannetti, S. Lloyd, and L. Maccone, Advances in quantum metrology, *Nat. Photon.* **5**, 222 (2011).
- [32] M. A. Taylor and W. P. Bowen, Quantum metrology and its application in biology, *Phys. Rep.* **615**, 1 (2016).
- [33] P.-A. Moreau, E. Toninelli, T. Gregory, and M. J. Padgett, Imaging with quantum states of light, *Nat. Rev. Phys.* **1**, 367 (2019).
- [34] S. Mukamel, M. Freyberger, W. Schleich, M. Bellini, A. Zavatta, G. Leuchs, C. Silberhorn, R. W. Boyd, L. L. Sánchez-Soto, A. Stefanov, *et al.*, Roadmap on quantum light spectroscopy, *J. Phys. B: At. Mol. Opt. Phys.* **53**, 072002 (2020).
- [35] R. Schnabel, N. Mavalvala, D. E. McClelland, and P. K. Lam, Quantum metrology for gravitational wave astronomy, *Nat. Commun.* **1**, 121 (2010).
- [36] J. Aasi, J. Abadie, B. P. Abbott, R. Abbott, T. D. Abbott, M. R. Abernathy, C. Adams, T. Adams, P. Addesso, R. X. Adhikari, *et al.*, Enhanced sensitivity of the LIGO gravitational wave detector by using squeezed states of light, *Nat. Photon* **7**, 613 (2013).
- [37] M. Tse, H. Yu, N. Kijbunchoo, A. Fernandez-Galiana, P. Dupej, L. Barsotti, C. D. Blair, D. D. Brown, S. E. Dwyer, A. Effler, *et al.*, Quantum-enhanced advanced LIGO detectors in the era of gravitational-wave astronomy, *Phys. Rev. Lett.* **123**, 231107 (2019).
- [38] H. Yu, L. McCuller, M. Tse, N. Kijbunchoo, L. Barsotti, and N. Mavalvala, Quantum correlations between light and the kilogram-mass mirrors of LIGO, *Nature* **583**, 43 (2020).
- [39] A. J. Kerman, Quantum information processing using quasiclassical electromagnetic interactions between qubits and electrical resonators, *New J. Phys.* **15**, 123011 (2013).
- [40] P.-M. Billangeon, J. S. Tsai, and Y. Nakamura, Circuit-QED-based scalable architectures for quantum information processing with superconducting qubits, *Phys. Rev. B* **91**, 094517 (2015).
- [41] N. Didier, J. Bourassa, and A. Blais, Fast quantum non-demolition readout by parametric modulation of longitudinal qubit-oscillator interaction, *Phys. Rev. Lett.* **115**, 203601 (2015).
- [10] F. Beaudoin, D. Lachance-Quirion, W. A. Coish, and M. Pioro-Ladrière, Coupling a single electron spin to a microwave resonator: controlling transverse and longitudinal couplings, *Nanotechnology* **27**, 464003 (2016).
- [43] S. Richer and D. DiVincenzo, Circuit design implementing longitudinal coupling: A scalable scheme for superconducting qubits, *Phys. Rev. B* **93**, 134501 (2016).
- [44] S. Richer, N. Maleeva, S. T. Skacel, I. M. Pop, and D. DiVincenzo, Inductively shunted transmon qubit with tunable transverse and longitudinal coupling, *Phys. Rev. B* **96**, 174520 (2017).
- [45] S. P. Harvey, C. G. L. Böttcher, L. A. Orona, S. D. Bartlett, A. C. Doherty, and A. Yacoby, Coupling two spin qubits with a high-impedance resonator, *Phys. Rev. B* **97**, 235409 (2018).
- [46] N. Lambert, M. Cirio, M. Delbecq, G. Allison, M. Marx, S. Tarucha, and F. Nori, Amplified and tunable transverse and longitudinal spin-photon coupling in hybrid circuit-QED, *Phys. Rev. B* **97**, 125429 (2018).
- [47] S. Bosco, P. Scarlino, J. Klinovaja, and D. Loss, Fully tunable longitudinal spin-photon interactions in Si and Ge quantum dots, *Phys. Rev. Lett.* **129**, 066801 (2022).
- [48] C. G. L. Böttcher, S. P. Harvey, S. Fallahi, G. C. Gardner, M. J. Manfra, U. Vool, S. D. Bartlett, and A. Yacoby, Parametric longitudinal coupling between a high-impedance superconducting resonator and a semiconductor quantum dot singlet-triplet spin qubit, *Nat. Commun.* **13**, 4773 (2022).
- [49] V. P. Michal, J. C. Abadillo-Uriel, S. Zihlmann, R. Maurand, Y.-M. Niquet, and M. Filippone, Tunable hole spin-photon interaction based on g-matrix modulation, *Phys. Rev. B* **107**, L041303 (2023).
- [50] Y. Fang, P. Philippopoulos, D. Culcer, W. A. Coish, and S. Chesi, Recent advances in hole-spin qubits, *Mater. Quantum. Technol.* **3**, 012003 (2023).
- [51] *See the Supplemental Material, which includes Refs. [80-90].*
- [52] A. H. Kiilerich and K. Mølmer, Input-output theory with quantum pulses, *Phys. Rev. Lett.* **123**, 123604 (2019).
- [53] A. H. Kiilerich and K. Mølmer, Quantum interactions with pulses of radiation, *Phys. Rev. A* **102**, 023717 (2020).
- [54] C. W. Gardiner and M. J. Collett, Input and output in damped quantum systems: Quantum stochastic differential equations and the master equation, *Phys. Rev. A* **31**, 3761 (1985).
- [55] J. Corrigan, B. Harpt, N. Holman, R. Ruskov, P. Marciniak, D. Rosenberg, D. Yost, R. Das, W. D. Oliver, R. McDermott, *et al.*, Longitudinal coupling between a Si/SiGe quantum dot and an off-chip TiN resonator, arXiv preprint arXiv:2212.02736 (2022).
- [56] E. Waks and J. Vuckovic, Dipole-induced transparency in drop-filter cavity-waveguide systems, *Phys. Rev. Lett.* **96**, 153601 (2006).
- [57] A. Auffèves-Garnier, C. Simon, J.-M. Gérard, and J.-P. Poizat, Giant optical nonlinearity induced by a single two-level system interacting with a cavity in the Purcell regime, *Phys. Rev. A* **75**, 053823 (2007).

- [58] D. Englund, A. Faraon, I. Fushman, N. Stoltz, P. Petroff, and J. Vuckovic, Controlling cavity reflectivity with a single quantum dot, *Nature* **450**, 857 (2007).
- [59] H. I. Nurdin, M. R. James, and N. Yamamoto, Perfect single device absorber of arbitrary traveling single photon fields with a tunable coupling parameter: A QSDE approach, in *2016 IEEE 55th Conference on Decision and Control (CDC)* (IEEE, 2016) pp. 2513–2518.
- [60] J.-C. Besse, S. Gasparinetti, M. C. Collodo, T. Walter, P. Kurpiers, M. Pechal, C. Eichler, and A. Wallraff, Single-shot quantum nondemolition detection of individual itinerant microwave photons, *Phys. Rev. X* **8**, 021003 (2018).
- [61] S. Kono, K. Koshino, Y. Tabuchi, A. Noguchi, and Y. Nakamura, Quantum non-demolition detection of an itinerant microwave photon, *Nat. Phys.* **14**, 546 (2018).
- [62] B. Hacker, S. Welte, S. Daiss, A. Shaikat, S. Ritter, L. Li, and G. Rempe, Deterministic creation of entangled atom–light Schrödinger-cat states, *Nat. Photon.* **13**, 110 (2019).
- [63] J.-C. Besse, S. Gasparinetti, M. C. Collodo, T. Walter, A. Remm, J. Krause, C. Eichler, and A. Wallraff, Parity detection of propagating microwave fields, *Phys. Rev. X* **10**, 011046 (2020).
- [64] A. Dragan and K. Banaszek, Homodyne Bell’s inequalities for entangled mesoscopic superpositions, *Phys. Rev. A* **63**, 062102 (2001).
- [65] T. Yu and J. H. Eberly, Evolution from entanglement to decoherence of bipartite mixed “X” states, *arXiv preprint quant-ph/0503089* (2005).
- [66] S. A. Hill and W. K. Wootters, Entanglement of a pair of quantum bits, *Phys. Rev. Lett.* **78**, 5022 (1997).
- [67] W. K. Wootters, Entanglement of formation of an arbitrary state of two qubits, *Phys. Rev. Lett.* **80**, 2245 (1998).
- [68] W. K. Wootters, Entanglement of formation and concurrence, *Quantum Inf. Comput.* **1**, 27 (2001).
- [69] P. Stano and D. Loss, Review of performance metrics of spin qubits in gated semiconducting nanostructures, *Nat. Rev. Phys.* **4**, 672 (2022).
- [70] M. Kjaergaard, M. E. Schwartz, J. Braumüller, P. Krantz, J. I.-J. Wang, S. Gustavsson, and W. D. Oliver, Superconducting qubits: Current state of play, *Annu. Rev. Condens. Matter Phys.* **11**, 369 (2020).
- [71] S. L. Braunstein and C. M. Caves, Statistical distance and the geometry of quantum states, *Phys. Rev. A* **72**, 3439 (1994).
- [72] S. L. Braunstein, C. M. Caves, and G. J. Milburn, Generalized uncertainty relations: theory, examples, and Lorentz invariance, *Ann. Phys.* **247**, 135 (1996).
- [73] Z. M. McIntyre and W. A. Coish, In preparation.
- [74] M. D. Reed, B. R. Johnson, A. A. Houck, L. DiCarlo, J. M. Chow, D. I. Schuster, L. Frunzio, and R. J. Schoelkopf, Fast reset and suppressing spontaneous emission of a superconducting qubit, *Appl. Phys. Lett.* **96**, 203110 (2010).
- [75] J. E. Johnson, C. Macklin, D. H. Slichter, R. Vijay, E. B. Weingarten, J. Clarke, and I. Siddiqi, Heralded state preparation in a superconducting qubit, *Phys. Rev. Lett.* **109**, 050506 (2012).
- [76] K. Geerlings, Z. Leghtas, I. M. Pop, S. Shankar, L. Frunzio, R. J. Schoelkopf, M. Mirrahimi, and M. H. Devoret, Demonstrating a driven reset protocol for a superconducting qubit, *Phys. Rev. Lett.* **110**, 120501 (2013).
- [77] T. Kobayashi, T. Nakajima, K. Takeda, A. Noiri, J. Yoneda, and S. Tarucha, Feedback-based active reset of a spin qubit in silicon, *Npj Quantum Inf.* **9**, 52 (2023).
- [78] Z. McIntyre and W. A. Coish, Non-Markovian transient spectroscopy in cavity QED, *Phys. Rev. Res.* **4**, L042039 (2022).
- [79] P. M. Mutter and G. Burkard, Fingerprints of qubit noise in transient cavity transmission, *Phys. Rev. Lett.* **128**, 236801 (2022).
- [80] X. Mi, J. V. Cady, D. M. Zajac, P. W. Deelman, and J. R. Petta, Strong coupling of a single electron in silicon to a microwave photon, *Science* **355**, 156 (2017).
- [81] A. J. Landig, J. V. Koski, P. Scarlino, U. Mendes, A. Blais, C. Reichl, W. Wegscheider, A. Wallraff, K. Ensslin, and T. Ihn, Coherent spin–photon coupling using a resonant exchange qubit, *Nature* **560**, 179 (2018).
- [82] N. Samkharadze, G. Zheng, N. Kalhor, D. Brousse, A. Sammak, U. Mendes, A. Blais, G. Scappucci, and L. Vandersypen, Strong spin-photon coupling in silicon, *Science* **359**, 1123 (2018).
- [83] I. Seidler, T. Struck, R. Xue, N. Focke, S. Trellenkamp, H. Bluhm, and L. R. Schreiber, Conveyor-mode single-electron shuttling in Si/SiGe for a scalable quantum computing architecture, *npj Quantum information* **8**, 100 (2022).
- [84] L. Childress, A. Sørensen, and M. D. Lukin, Mesoscopic cavity quantum electrodynamics with quantum dots, *Phys. Rev. A* **69**, 042302 (2004).
- [85] K. D. Petersson, J. R. Petta, H. Lu, and A. C. Gosard, Quantum coherence in a one-electron semiconductor charge qubit, *Phys. Rev. Lett.* **105**, 246804 (2010).
- [86] R. Schoelkopf and S. Girvin, Wiring up quantum systems, *Nature* **451**, 664 (2008).
- [87] A. Imamoglu, Cavity QED based on collective magnetic dipole coupling: spin ensembles as hybrid two-level systems, *Phys. Rev. Lett.* **102**, 083602 (2009).
- [88] G. Burkard, T. D. Ladd, A. Pan, J. M. Nichol, and J. R. Petta, Semiconductor spin qubits, *Rev. Mod. Phys.* **95**, 025003 (2023).
- [89] Y. M. Zhang, X. W. Li, W. Yang, and G. R. Jin, Quantum Fisher information of entangled coherent states in the presence of photon loss, *Phys. Rev. A* **88**, 043832 (2013).
- [90] T. Yu and J. H. Eberly, Quantum open system theory: bipartite aspects, *Phys. Rev. Lett.* **97**, 140403 (2006).

Supplementary Material for ‘A photonic which-path entangler based on longitudinal cavity-qubit coupling’

Z. M. McIntyre and W. A. Coish

Department of Physics, McGill University, 3600 rue University, Montreal, QC, H3A 2T8, Canada

SI. CAVITY-QUBIT HAMILTONIAN

In general, the wavefunctions defining the ground and excited states of a qubit can be tuned through one or more parameters. For spin qubits in gate-defined double quantum dots, these could be gate voltages; for superconducting qubits, they could be fluxes. When these parameters are modulated in time, the Hamiltonian H_q of the qubit acquires a time dependence. The full cavity-qubit Hamiltonian can then be written as

$$H(t) = H_q(t) + \omega_c a^\dagger a + H_{\text{int}}, \quad (\text{S1})$$

where $H_q(t) |s(t)\rangle = \epsilon_s(t) |s(t)\rangle$ is the Hamiltonian whose low-energy instantaneous eigenstates (labelled by $s = 0, 1$) are used to encode the qubit, and where a annihilates an excitation in the cavity mode (whose frequency is denoted ω_c). In many architectures (involving e.g. atoms, excitons, or spins together with spin-orbit coupling), the cavity-qubit interaction H_{int} has its origins in the electric-dipole interaction $H_{\text{int}} = e \mathbf{E} \cdot \mathbf{r}$, where $e > 0$ is the magnitude of the electron charge, \mathbf{E} is the electric field of the cavity at the location of the dipole (qubit), and \mathbf{r} is the position operator of an electron.

We transform $H(t)$ [Eq. (S1)] via the unitary transformation $U(t) = \sum_s |s\rangle \langle s(t)|$ to the instantaneous adiabatic eigenbasis, in which

$$\tilde{H}(t) = U(t)H(t)U^\dagger(t) - iU(t)\dot{U}^\dagger(t). \quad (\text{S2})$$

So far, this transformation is exact. Treating the evolution of the system within an adiabatic approximation,

$$\tilde{H}(t) \simeq \tilde{H}_{\text{adiabatic}}(t) = U(t)H(t)U^\dagger(t), \quad (\text{S3})$$

requires that the usual adiabaticity condition be satisfied,

$$\frac{|\langle \bar{s}(t) | \partial_t | s(t) \rangle|}{|\epsilon_0(t) - \epsilon_1(t)|} \ll 1, \quad (\text{S4})$$

where $s \in \{0, 1\}$, $\bar{1} = 0$, and $\bar{0} = 1$. A similar condition must also be obeyed by proximal excited states. In particular, since we consider modulation at the cavity frequency ω_c , there should be no coupled excited states at (or near) the cavity resonance. The cavity electric field is quantized $\mathbf{E} = i\mathbf{E}_0(a^\dagger - a)$, giving

$$\tilde{H}_{\text{adiabatic}}(t) = \epsilon_0(t) |0\rangle \langle 0| + \epsilon_1(t) |1\rangle \langle 1| + \omega_c a^\dagger a + i \sum_{s=0,1} g_s(t) |s\rangle \langle s| (a^\dagger - a) + i \sum_s g_\perp(t) |s\rangle \langle \bar{s}| (a^\dagger - a), \quad (\text{S5})$$

where the longitudinal coupling $g_s(t) = e\mathbf{E}_0 \cdot \langle s(t) | \mathbf{r} | s(t) \rangle$ depends on the s -dependent electric dipole moment $-e \langle s(t) | \mathbf{r} | s(t) \rangle$, and where the transverse coupling $g_\perp(t) = e\mathbf{E}_0 \cdot \langle s(t) | \mathbf{r} | \bar{s}(t) \rangle$ depends on the transition dipole moment $-e \langle s(t) | \mathbf{r} | \bar{s}(t) \rangle$. When the transition dipole is weak, or for a qubit strongly detuned from the cavity, the transverse term may be strongly suppressed, yielding an interaction that is predominantly longitudinal.

We assume that $g_0(t)$ and $g_1(t)$ can both be tuned by varying parameters $x_j(t)$. (These could be local potentials or electric fields for atomic, exciton, or spin qubits, or they could be fluxes for flux-biased superconducting qubits.) To linear order,

$$g_s(t) = \bar{g}_s + \delta g_s(t) \simeq \bar{g}_s + \sum_j \frac{\partial g_s}{\partial x_j} \delta x_j(t), \quad (\text{S6})$$

where $\delta g_s(t)$ describes a time-dependent modulation of $g_s(t) = \bar{g}_s + \delta g_s(t)$ [and similarly for $\delta x_i(t)$].

When one of $g_s(t)$ (for $s = 0, 1$) can be modulated independently of the other with a single $x_j(t)$, the required time-dependent modulation can be realized directly. More generally, it may be necessary to consider control through a minimum of two parameters $x_j(t)$ ($j = 0, 1$). Realizing the time-dependence of $g_s(t)$ required for the entangler then calls for a solution to the system of equations

$$\begin{pmatrix} \delta x_0 \\ \delta x_1 \end{pmatrix} = \mathbf{J}^{-1} \begin{pmatrix} \delta g_0(t) \\ \delta g_1(t) \end{pmatrix} = \mathbf{J}^{-1} \begin{pmatrix} 0 \\ 2|\tilde{g}_1(t)| \cos[\omega_c t - \vartheta(t)] \end{pmatrix}, \quad (\text{S7})$$

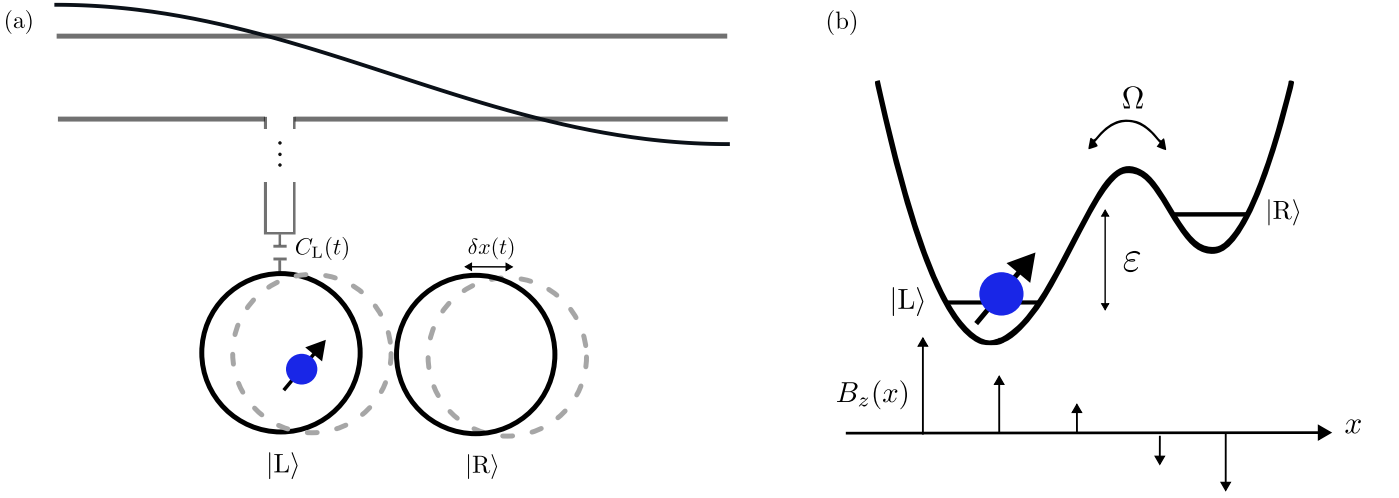


FIG. S3. (a) An electron in a double quantum dot can be coupled capacitively to a microwave resonator via a metallic finger (vertical gray rectangle) located near one of the dots. We assume that the dot-to-finger lever arm $\alpha_L \propto C_L$ of the left dot can be modulated by shifting the position $x(t)$ of the orbitals $\psi_l(\mathbf{r}, t)$ ($l = L, R$) of the individual dots through a gate voltage modulation. (b) A spin qubit in a double quantum dot: A magnetic field gradient $B_z(x)$ across the double-dot axis can be used to couple the electron spin and charge (orbital) degrees of freedom. The electron spin can then couple to the resonator via an interaction of the form given in Eq. (S16).

where here, \mathbf{J} is a 2×2 matrix with elements $J_{sj} = \partial g_s / \partial x_j$, and where $\tilde{g}_1(t) = e^{i\vartheta(t)} |\tilde{g}_1(t)|$ varies slowly relative to the timescale ω_c^{-1} . A sufficient condition for Eq. (S7) to have a nontrivial solution is that \mathbf{J}^{-1} be defined, i.e. that the determinant of \mathbf{J} be nonvanishing.

We assume that the modulations of $\delta x_j(t)$ prescribed by Eq. (S7) have a negligible impact on $\epsilon_s(t) \simeq \epsilon_s$, so that, neglecting the transverse coupling term ($\propto g_\perp$) and up to a constant shift in energy,

$$\tilde{H}_{\text{adiabatic}}(t) \simeq \frac{1}{2} \omega'_q \sigma_z + \omega_c a^\dagger a + i g_0 |0\rangle \langle 0| (a^\dagger - a) + i g_1(t) |1\rangle \langle 1| (a^\dagger - a), \quad (\text{S8})$$

where here, $\sigma_z = |0\rangle \langle 0| - |1\rangle \langle 1|$ and $\omega'_q = \epsilon_0 - \epsilon_1$.

We now perform a polaron transformation $\tilde{\tilde{H}}(t) = e^S \tilde{H}_{\text{adiabatic}}(t) e^{-S}$ on Eq. (S8), where

$$S = i \frac{g_0}{\omega_c} |0\rangle \langle 0| (a^\dagger - a). \quad (\text{S9})$$

Up to a constant shift in energy, the result of this transformation is

$$\tilde{\tilde{H}}(t) = \frac{1}{2} \omega_q \sigma_z + \omega_c a^\dagger a + i g_1(t) |1\rangle \langle 1| (a^\dagger - a), \quad (\text{S10})$$

where here, $\omega_q = \omega'_q - g_0^2 / 2\omega_c$ is the qubit frequency accounting for the polaron shift. To model the effects of dephasing, we assume that the qubit splitting ω_q in Eq. (S10) is subject to classical fluctuations described by a stochastic noise process $\xi(t)$: $\omega_q \rightarrow \omega_q + \xi(t)$. Transforming Eq. (S10) to an interaction picture with respect to $\omega_q \sigma_z / 2 + \omega_c a^\dagger a$ and performing a rotating-wave approximation then recovers Eq. (1) of the main text.

A. Physical examples

In this section, we derive the form of the longitudinal coupling between a microwave cavity constructed from a superconducting stripline resonator and a qubit encoded in either the charge or spin states of an electron in a double quantum dot (Fig. S3). In each case (charge or spin qubits), we find the conditions under which the coupling can be modulated for only one of the qubit states [giving a form $\propto g_1(t) |1\rangle \langle 1|$ with $\delta g_0(t) = 0$], as required for the which-path entangler.

The interaction between the charge density operator $\rho(\mathbf{r})$ for a qubit and the electric potential $V(\mathbf{r}, t)$ due to a resonator can be written as

$$H_\rho = \int d^3r \rho(\mathbf{r}) V(\mathbf{r}, t). \quad (\text{S11})$$

When the potential $V(\mathbf{r}, t)$ is a slowly-varying function of \mathbf{r} on the scale of the qubit charge distribution, it can be expanded about the location \mathbf{r}_0 of the qubit, giving the electric dipole approximation (in the length gauge):

$$H_\rho \simeq QV(\mathbf{r}_0, t) - \mathbf{d} \cdot \mathbf{E}(\mathbf{r}_0, t). \quad (\text{S12})$$

Here, $\mathbf{E}(\mathbf{r}_0, t) = -\nabla V(\mathbf{r}_0, t)$ is the cavity electric field at the position of the qubit. The quantities Q and \mathbf{d} are the total charge and dipole operators, respectively:

$$Q = \int d^3r \rho(\mathbf{r}); \quad \mathbf{d} = \int d^3r \rho(\mathbf{r})(\mathbf{r} - \mathbf{r}_0). \quad (\text{S13})$$

For qubit states constructed from systems with overall charge neutrality (e.g., neutral atoms and excitons), $Q \simeq 0$. An effective qubit-cavity interaction can then be derived by quantizing the cavity field and forming matrix elements of the dipole operator, as described in the main text and in Sec. SI, above. Since the dipole operator is odd under inversion about \mathbf{r}_0 ($\mathbf{d} \rightarrow -\mathbf{d}$), the longitudinal coupling will vanish for these systems (within the dipole approximation) if the qubit eigenstates $|s\rangle$ have definite parity under inversion. This will be the case for high-symmetry free-atom eigenstates, but it will not generally be true for lower-symmetry designed systems like the quantum dots considered here.

1. Charge qubit in a double quantum dot

In contrast to the far-field approach described above, many experiments that couple quantum dots to superconducting resonators instead exploit the strong near-field coupling of a quantum-dot charge to a metallic gate that extends from the resonator to the vicinity of the quantum dot [S1–S3] (Fig. S3). For these systems, it is important to work directly from Eq. (S11) to find an accurate microscopic description of the coupling. To simplify the effective coupling, we now consider only a single quantized resonator mode. We further project the charge density operator onto the lowest two (left/right) orbital states of a double quantum dot. Thus, we approximate

$$V(\mathbf{r}, t) \simeq i\phi_0(\mathbf{r})V_0(a^\dagger e^{i\omega_c t} - a e^{-i\omega_c t}), \quad (\text{S14})$$

$$\rho(\mathbf{r}, t) \simeq -e|\psi_L(\mathbf{r}, t)|^2 |L\rangle \langle L| - e|\psi_R(\mathbf{r}, t)|^2 |R\rangle \langle R|, \quad (\text{S15})$$

where the dimensionless mode function $\phi_0(\mathbf{r})$ solves Poisson's equation subject to the device geometry. Here, V_0 is the amplitude of zero-point voltage fluctuations in the resonator itself, and $\psi_l(\mathbf{r}, t)$ ($l = L, R$) is the envelope function for quantum dot l . We assume that the quantum-dot orbitals can be manipulated via external gate voltages, leading to adiabatically varying time-dependent envelope functions. This has been achieved in experiments on shuttling electrons between quantum dots [S4].

The coupling to the right dot $|R\rangle$ is negligible if $\phi_0(\mathbf{r})$ is vanishingly small wherever the envelope function $\psi_R(\mathbf{r}, t)$ has significant weight. In this limit, we insert Eqs. (S14) and (S15) into Eq. (S11), giving the coupling between a double-dot charge qubit and a microwave resonator [S5],

$$e^{-i\omega_c a^\dagger at} H_\rho e^{i\omega_c a^\dagger at} \simeq H_{\text{int}} = ig_c(t) |L\rangle \langle L| (a^\dagger - a), \quad g_c(t) = -e\alpha_L(t)V_0. \quad (\text{S16})$$

The coupling $g_c(t)$ between the charge and the resonator can thus be controlled through the lever arm $\alpha_L(t)$, which can itself be controlled via the left dot orbital:

$$\alpha_L(t) = \int d^3r \phi_0(\mathbf{r}) |\psi_L(\mathbf{r}, t)|^2, \quad (\text{S17})$$

$$\alpha_R(t) = \int d^3r \phi_0(\mathbf{r}) |\psi_R(\mathbf{r}, t)|^2 \simeq 0. \quad (\text{S18})$$

By manipulating the shape, size, and position of the left quantum dot via gate voltages, α_L can therefore be modulated. The lever arm α_L can equivalently be written in terms of the capacitance C_L between the left dot and the resonator [Fig. S3(a)] and the total capacitance C_Σ of the left dot [S5]:

$$\alpha_L = \frac{C_L}{C_\Sigma}. \quad (\text{S19})$$

For a charge qubit encoded in the left/right basis ($|L\rangle \rightarrow |1\rangle$, $|R\rangle \rightarrow |0\rangle$), Eq. (S16) directly achieves the form of longitudinal coupling required for the which-path entangler, where $g_c(t) \rightarrow g_1(t)$, and where $g_0(t) \simeq 0$ provided the

cross-capacitance between the resonator and the right dot is negligible [equivalently, provided Eq. (S18) is satisfied]. Charge qubits of this type are sensitive to electric field fluctuations, leading to coherence times typically in the range of $T_2^* \sim 100$ ps-10 ns [S6]. These short coherence times would likely limit the applicability of pure charge qubits to the entangler scheme presented in the main text. For this reason, in the next section we consider longitudinal coupling for a spin qubit, since spin qubits typically have longer coherence times.

2. Spin qubit in a double quantum dot

An interaction of the form given in Eq. (S16) can also be used to generate coupling between a microwave resonator and an electron spin. This generally requires coupling of the spin and charge degrees-of-freedom, since direct magnetic coupling of the electron spin magnetic moment to the resonator magnetic field is typically weak, on the order of a few tens of Hz [S7, S8]. In the absence of intrinsic spin-orbit coupling, a synthetic spin-orbit interaction can be generated from a magnetic field gradient across the two dots [S9] [Fig. S3(b)]. For a magnetic field oriented along the z axis, the Hamiltonian describing spin-charge hybridization is given by [S10]

$$H_q(t) = \frac{1}{2}[\varepsilon\tau_z + \Omega(t)\tau_x] + \frac{1}{2}(b_L|L\rangle\langle L| + b_R|R\rangle\langle R|)\sigma_z, \quad (\text{S20})$$

where σ_z is the Pauli-Z operator of the spin, ε is the double-dot detuning controlling the relative dot potentials [Fig. S3(b)], and where $b_{L,R} = g^*\mu_B \int d^3r |\psi_{L,R}(\mathbf{r})|^2 B_z(\mathbf{r})$. Here, g^* is the (material-dependent) electron g -factor and μ_B is the Bohr magneton. The tunnel splitting $\Omega(t)$ can be controlled through a gate voltage and will be used to modulate the coupling. In Eq. (S20), we have also introduced the orbital pseudospin Pauli operators

$$\tau_x = |L\rangle\langle R| + |R\rangle\langle L|, \quad (\text{S21})$$

$$\tau_z = |R\rangle\langle R| - |L\rangle\langle L|. \quad (\text{S22})$$

Equation (S20) can be diagonalized conditioned on the spin state $|\sigma\rangle$ (where $\sigma = \uparrow, \downarrow$ with $\sigma_z|\sigma\rangle = \pm|\sigma\rangle$), giving

$$\begin{aligned} |+, \sigma\rangle_t &= \cos\frac{\theta_\sigma(t)}{2} |R\rangle|\sigma\rangle + \sin\frac{\theta_\sigma(t)}{2} |L\rangle|\sigma\rangle, \\ |-, \sigma\rangle_t &= -\sin\frac{\theta_\sigma(t)}{2} |R\rangle|\sigma\rangle + \cos\frac{\theta_\sigma(t)}{2} |L\rangle|\sigma\rangle, \end{aligned} \quad (\text{S23})$$

where $\tan\theta_{\uparrow,\downarrow}(t) = \Omega(t)/[\varepsilon \pm \Delta b_z]$ for $\Delta b_z = (b_R - b_L)/2$. When the Zeeman energy is small compared to the double-dot orbital energy, the lowest two energy eigenstates are predominantly distinguished by spin $\sigma = \uparrow, \downarrow$, but they will also have slightly different charge distributions. The two states $|-, \sigma\rangle_t$ then encode the qubit:

$$|0(t)\rangle = |-, \uparrow\rangle_t, \quad (\text{S24})$$

$$|1(t)\rangle = |-, \downarrow\rangle_t. \quad (\text{S25})$$

In order to obtain an effective qubit-resonator interaction, we now project Eq. (S16) (with a time-independent g_c) into the qubit subspace and transform to the instantaneous adiabatic eigenbasis via the unitary $U = \sum |s\rangle\langle s(t)|$ (as described in Sec. SI), giving

$$H_{\text{int}}^{\text{eff}}(t) = UP(t)H_{\text{int}}P(t)^\dagger U^\dagger = ig_0(t)|0\rangle\langle 0|(a^\dagger - a) + ig_1(t)|1\rangle\langle 1|(a^\dagger - a), \quad P(t) = \sum_\sigma |-, \sigma\rangle_t\langle -, \sigma|, \quad (\text{S26})$$

where

$$\begin{aligned} g_0(t) &= g_c \cos^2 \frac{\theta_\uparrow(t)}{2} = \frac{g_c}{2} \left(1 + \frac{\varepsilon + \Delta b_z}{\sqrt{(\varepsilon + \Delta b_z)^2 + \Omega^2(t)}} \right), \\ g_1(t) &= g_c \cos^2 \frac{\theta_\downarrow(t)}{2} = \frac{g_c}{2} \left(1 + \frac{\varepsilon - \Delta b_z}{\sqrt{(\varepsilon - \Delta b_z)^2 + \Omega^2(t)}} \right). \end{aligned} \quad (\text{S27})$$

For $\varepsilon = -\Delta b_z$, we then have $g_0 = g_c/2$ (time-independent) for all finite values of the tunnel splitting $\Omega(t)$. Hence for this choice of parameters ($\varepsilon = -\Delta b_z$), modulating $\Omega(t)$ only affects the coupling of the resonator to state $|1\rangle$:

$$g_0 = \frac{g_c}{2}, \quad (\text{S28})$$

$$g_1(t) = \frac{g_c}{2} \left(1 - \frac{2\Delta b_z}{\sqrt{4\Delta b_z^2 + \Omega^2(t)}} \right). \quad (\text{S29})$$

For $\Omega(t) = \bar{\Omega} + \delta\Omega(t)$ with $\bar{\Omega} \gg |\Delta b_z|, |\delta\Omega(t)|$, we then have $g_1(t) = \bar{g}_1 + \delta g_1(t)$, where

$$\delta g_1(t) \simeq \frac{g_c \Delta b_z}{\bar{\Omega}^2} \delta\Omega(t). \quad (\text{S30})$$

SII. FINITE-BANDWIDTH CORRECTIONS TO IDEALIZED QWP STATES

In this section, we quantify finite-bandwidth effects due to a finite duration of the input wavepacket $u(t)$. These corrections lead to imperfect transmission and reflection of the incident wavepacket for a qubit prepared in the state $|0\rangle$, leading to deviations from the idealized QWP states considered in the main text.

For a qubit initialized in $|+\rangle = (|1\rangle + |0\rangle)/\sqrt{2}$, the QWP state generated for an incident coherent state with amplitude α_0 is given by Eq. (7) of the main text (here we consider the case $\xi = 0$ since dephasing does not affect the present discussion):

$$|\Psi\rangle = \frac{1}{\sqrt{2}} (|1, \psi_1\rangle + |0, \psi_0\rangle), \quad (\text{S31})$$

where for $s = 0, 1$,

$$|\psi_s\rangle = \prod_{i=1,2} D_i(\alpha_{is}) |\text{vac}\rangle. \quad (\text{S32})$$

Here, $|\text{vac}\rangle$ is the vacuum, $D_i(\alpha) = e^{\alpha a_{v_i}^\dagger - \text{h.c.}}$ is a displacement operator that generates a coherent state with amplitude α in mode a_{v_i} , and

$$\alpha_{is} = (-1)^{i-1} \alpha_0 \int_0^\infty dt |v_i(t)|^2 = (-1)^{i-1} \alpha_0 \int \frac{d\omega}{2\pi} |v_i(\omega)|^2 \quad (\text{S33})$$

is the qubit-state-dependent stationary amplitude of the coherent state in mode a_{v_i} . The reflected (v_1) and transmitted (v_2) pulses are given by $v_1(\omega) = R(\omega)u(\omega)$ and $v_2(\omega) = T(\omega)u(\omega)$, respectively, where $R(\omega)$ and $T(\omega)$ are the reflection and transmission coefficients, and where $u(\omega)$ is the waveform of the input pulse. The input pulse is assumed to have a duration $\sim \tau$.

Up to corrections that vanish for $\kappa\tau \rightarrow \infty$, only one of α_{is} is nonzero for each value of s , provided

$$\kappa_1 = \kappa_2 = \frac{\kappa}{2}. \quad (\text{S34})$$

With this choice of $\kappa_{1,2}$, Eq. (S31) describes a coherent state whose which-path degree-of-freedom is entangled with the qubit: For a qubit in state $|1\rangle$, the incident coherent state is fully reflected, whereas for a qubit in state $|0\rangle$, it is fully transmitted, up to corrections that vanish for $\kappa\tau \rightarrow \infty$. In order to quantify these corrections, we consider the fidelity $F = |\langle \Psi_\infty | \Psi_{\kappa\tau} \rangle|^2$ of the idealized QWP state $|\Psi_\infty\rangle$ having ideal which-path character, obtained by taking $\kappa\tau \rightarrow \infty$, relative to the QWP state $|\Psi_{\kappa\tau}\rangle$ obtained for finite $\kappa\tau$. This is easily accomplished using the relation $R(\omega) - 1 = T(\omega)$ that follows from input-output theory after setting $\kappa_1 = \kappa_2 = \kappa/2$, together with Eq. (4) of the main text:

$$T(\omega) = (1 - s) \frac{\kappa/2}{i\omega - \kappa/2}. \quad (\text{S35})$$

From Eq. (S33), we then have $\alpha_{11} = \alpha_0$, $\alpha_{21} = 0$, as well as the non-trivial coherent-state amplitudes

$$\alpha_{10} = \alpha_0 \int \frac{d\omega}{2\pi} |u(\omega)|^2 \times \frac{\omega^2}{\omega^2 + \kappa^2/4}, \quad (\text{S36})$$

$$\alpha_{20} = -\alpha_0 \int \frac{d\omega}{2\pi} |u(\omega)|^2 \times \frac{\kappa^2/4}{\omega^2 + \kappa^2/4}, \quad (\text{S37})$$

which depend on $u(\omega)$. Since the state $|1, \psi_1\rangle$ appearing in Eq. (S31) describes a perfectly reflected wavepacket for any $\kappa\tau$, the fidelity F is controlled entirely by $|0, \psi_0\rangle$, where ideally (i.e. for $\kappa\tau \rightarrow \infty$), $|\psi_0\rangle = D_2(\alpha_0) |\text{vac}\rangle$. The fidelity is therefore given by

$$F = \frac{1}{4} \left| 1 + e^{-\frac{1}{2}|\alpha_0|^2} e^{\alpha_0^* \alpha_{20}} \prod_{i=1,2} e^{-\frac{1}{2}|\alpha_{i0}|^2} \right|^2, \quad (\text{S38})$$

where $|\Psi_0\rangle = |0, -\alpha_p\rangle$ and $|\Psi_1\rangle = |1, +\alpha_p\rangle$ for $\alpha_p = \alpha_0[(1-p)/2]^{1/2}$, and where for zero-mean, Gaussian, stationary noise having spectral density $S(\omega) = \int dt e^{-i\omega t} \langle \xi(t)\xi \rangle$,

$$\chi_\xi(t) = \int \frac{d\omega}{2\pi} \frac{4\sin^2(\frac{\omega t}{2})}{\omega^2} S(\omega). \quad (\text{S46})$$

The photonic degree-of-freedom can then be entangled with a second qubit, initialized in $|+\rangle$, through an interaction that imparts a phase shift sending $|+\rangle \rightarrow |-\rangle$, conditioned on the electric field having an odd photon-number parity [S12–S15]. The photon-number parity can be identified by re-expressing $|\pm\alpha_p\rangle$ in terms of the even- and odd-parity cat states $|C_\pm\rangle = N_\pm(|+\alpha_p\rangle \pm |-\alpha_p\rangle)$, where $N_\pm = (2 \pm 2e^{-2|\alpha_p|^2})^{-1/2}$. In addition to the approaches presented in Refs. S12–S15, the required parity-conditioned phase flip could also be implemented by reflecting the incoming field off a single-sided cavity dispersively coupled to a qubit, i.e., coupled through an interaction of the form $\chi\sigma_z a^\dagger a$. In that case, the reflection coefficient (where ω is relative to the bare cavity frequency) is given by

$$R(\omega) = \frac{i(z\chi - \omega) - \kappa/2}{i(z\chi - \omega) + \kappa/2}, \quad (\text{S47})$$

where $z = +1$ ($z = -1$) for a qubit in state $|1\rangle$ ($|0\rangle$). In this setup, an input coherent state occupying a spatiotemporal mode of duration τ , resonant with χ (corresponding to the cavity frequency conditioned on the qubit being in state $|1\rangle$), will acquire a π phase shift (sending $|\pm\alpha\rangle \rightarrow |\mp\alpha\rangle$) provided $\kappa\tau$ is large. With the qubit in state $|0\rangle$, however, and provided $2|\chi| \gg \kappa$, where κ is the cavity decay rate (requiring that $\chi \gg \kappa \gg 1/\tau$), the same field will be far off resonance and will therefore be reflected without a phase shift.

Homodyne detection of the electric field quadrature along the axis of coherent-state displacement can be described by the two-element positive operator-valued measure (POVM) $P_\pm = (1 \pm C_\theta)/2$, where θ (not to be confused with θ_ξ , defined above) is the phase of $\alpha_p = e^{i\theta}|\alpha_p|$, and where [S16]

$$C_\theta = \int_0^\infty dx H_\theta(x) - \int_{-\infty}^0 dx H_\theta(x), \quad H_\theta(x) = \frac{1}{\sqrt{\pi(1-\eta)}} \exp\left\{-\frac{(x/\sqrt{\eta} - \hat{x}_\theta)^2}{1/\eta - 1}\right\}. \quad (\text{S48})$$

Here, η is the detection efficiency and $\hat{x}_\theta = (e^{i\theta}a_+^\dagger + e^{-i\theta}a_+)/\sqrt{2}$. The operator C_θ [Eq. (S48)] has the following symmetries with respect to $|\pm\alpha_p\rangle$ [S16]:

$$\langle \alpha_p | C_\theta | \alpha_p \rangle = -\langle -\alpha_p | C_\theta | -\alpha_p \rangle = \text{erf}(\sqrt{2\eta}|\alpha_p|) \quad (\text{S49})$$

$$\langle \alpha_p | C_\theta | -\alpha_p \rangle = \langle -\alpha_p | C_\theta | \alpha_p \rangle = 0. \quad (\text{S50})$$

We define Krauss operators K_\pm given by $K_\pm = U\sqrt{1 \pm C_\theta}$, where U is a unitary. This can be done since $\|C_\theta\| \leq 1$. The post-measurement state of the qubits can then be written as

$$\tilde{\varrho}_\pm(t) = \frac{\text{Tr}_{a_+}\{K_\pm \varrho(t) K_\pm^\dagger\}}{\text{Tr}\{K_\pm^\dagger K_\pm \varrho(t)\}}, \quad (\text{S51})$$

where $\text{Tr}_{a_+}\{\dots\}$ denotes a partial trace over the state of the a_+ mode. Using the symmetries of C_θ given in Eqs. (S49) and (S50), we then find that

$$\tilde{\varrho}_\pm(t) = p_\pm \varrho_+(t) + p_\mp \varrho_-(t), \quad (\text{S52})$$

where $p_\pm = \frac{1}{2}[1 \pm \text{erf}(\sqrt{2\eta}|\alpha_p|)]$, and where the states $\varrho_\pm(t)$ are given by $2\varrho_\pm(t) = (1 \pm \sigma_z \sigma_z) + e^{-pN - \chi_\xi(t)}(\sigma_x \sigma_x \mp \sigma_y \sigma_y)$. In the computational basis $\{|0, 0\rangle, |0, 1\rangle, |1, 0\rangle, |1, 1\rangle\}$, these can be written in matrix form as

$$\varrho_+(t) = \frac{1}{2} \begin{pmatrix} 1 & 0 & 0 & e^{-pN - \chi_\xi(t)} \\ 0 & 0 & 0 & 0 \\ 0 & 0 & 0 & 0 \\ e^{-pN - \chi_\xi(t)} & 0 & 0 & 1 \end{pmatrix}, \quad \varrho_-(t) = \frac{1}{2} \begin{pmatrix} 0 & 0 & 0 & 0 \\ 0 & 1 & e^{-pN - \chi_\xi(t)} & 0 \\ 0 & e^{-pN - \chi_\xi(t)} & 1 & 0 \\ 0 & 0 & 0 & 0 \end{pmatrix}. \quad (\text{S53})$$

Note that in the absence of both dephasing and photon loss ($p = \xi = 0$), the above states are Bell states: $\varrho_\pm = (|+, +\rangle \pm |-, -\rangle)/\sqrt{2}$ for $|\pm\rangle = (|1\rangle \pm |0\rangle)/\sqrt{2}$.

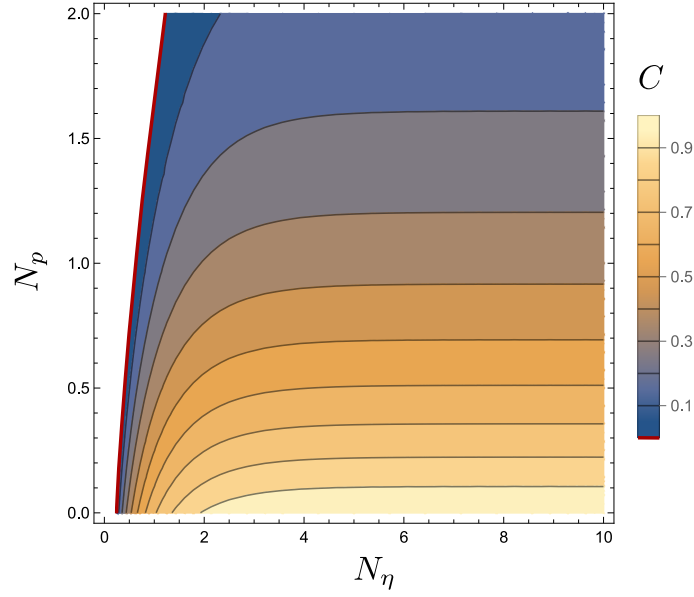


FIG. S4. Sudden death of entanglement: For each value of $N_\eta = \eta(1-p)N$, there is a critical threshold in $N_p = pN$ beyond which the two-qubit concurrence vanishes. The contour $C = 0$ is indicated in red.

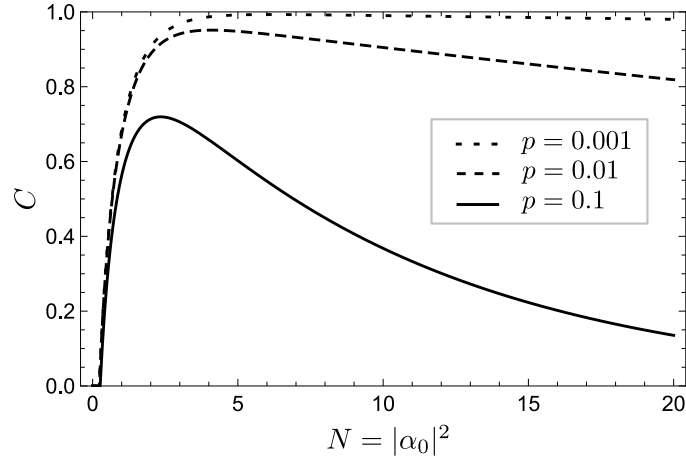


FIG. S5. The concurrence [Eq. (S55)] with $\xi(t) = 0$ and $\eta = 1$ for $p = 0.001$ (dotted line), $p = 0.01$ (dashed line), and $p = 0.1$ (solid line).

Given Eq. (S53), it is easily seen that $\tilde{\varrho}_\pm(t)$ is an X state [S17, S18], so called because its nonzero entries form an ‘X’ shape. For an X state of the form

$$\begin{pmatrix} a & 0 & 0 & w \\ 0 & b & z & 0 \\ 0 & z^* & c & 0 \\ w^* & 0 & 0 & d \end{pmatrix}, \quad (\text{S54})$$

where $a + b + c + d = 1$, the concurrence C [S19–S21] is easy to calculate [S17]: $C = 2\max\{0, |z| - \sqrt{ad}, |w| - \sqrt{bc}\}$. For $\tilde{\varrho}_\pm(t)$, this gives $C(t) = \max\{0, (1 - \delta)e^{-pN - \chi_\xi(t)} - \delta\}$, where $\delta = p_- = \text{erfc}(\sqrt{2\eta}|\alpha_p|)/2$. In terms of $N_\eta = \eta(1-p)N$ and $N_p = pN$, this result can be written as

$$C(t) = \max\{0, \text{erf}(\sqrt{N_\eta})e^{-N_p - \chi_\xi(t)} - \text{erfc}(\sqrt{N_\eta})\}. \quad (\text{S55})$$

This recovers Eq. (8) of the main text. We plot the concurrence as a function of N_η and N_p with $\xi(t) = 0$ (Fig. S4)

in order to illustrate the sudden death of entanglement. In Fig. S5, we plot C as a function of N for $\eta = 1$ in order to illustrate that for any fixed value of p , there exists a value of N such that the concurrence is maximized.

* zoe.mcintyre@mail.mcgill.ca

† william.coish@mcgill.ca

- [S1] X. Mi, J. V. Cady, D. M. Zajac, P. W. Deelman, and J. R. Petta, Strong coupling of a single electron in silicon to a microwave photon, *Science* **355**, 156 (2017).
- [S2] A. J. Landig, J. V. Koski, P. Scarlino, U. Mendes, A. Blais, C. Reichl, W. Wegscheider, A. Wallraff, K. Ensslin, and T. Ihn, Coherent spin-photon coupling using a resonant exchange qubit, *Nature* **560**, 179 (2018).
- [S3] N. Samkharadze, G. Zheng, N. Kalhor, D. Brousse, A. Sammak, U. Mendes, A. Blais, G. Scappucci, and L. Vandersypen, Strong spin-photon coupling in silicon, *Science* **359**, 1123 (2018).
- [S4] I. Seidler, T. Struck, R. Xue, N. Focke, S. Trellenkamp, H. Bluhm, and L. R. Schreiber, Conveyor-mode single-electron shuttling in Si/SiGe for a scalable quantum computing architecture, *npj Quantum Inf.* **8**, 100 (2022).
- [S5] L. Childress, A. Sørensen, and M. D. Lukin, Mesoscopic cavity quantum electrodynamics with quantum dots, *Phys. Rev. A* **69**, 042302 (2004).
- [S6] K. D. Petersson, J. R. Petta, H. Lu, and A. C. Gossard, Quantum coherence in a one-electron semiconductor charge qubit, *Phys. Rev. Lett.* **105**, 246804 (2010).
- [S7] R. Schoelkopf and S. Girvin, Wiring up quantum systems, *Nature* **451**, 664 (2008).
- [S8] A. Imamoglu, Cavity QED based on collective magnetic dipole coupling: spin ensembles as hybrid two-level systems, *Phys. Rev. Lett.* **102**, 083602 (2009).
- [S9] G. Burkard, T. D. Ladd, A. Pan, J. M. Nichol, and J. R. Petta, Semiconductor spin qubits, *Rev. Mod. Phys.* **95**, 025003 (2023).
- [S10] F. Beaudoin, D. Lachance-Quirion, W. A. Coish, and M. Pioro-Ladrière, Coupling a single electron spin to a microwave resonator: controlling transverse and longitudinal couplings, *Nanotechnology* **27**, 464003 (2016).
- [S11] Y. M. Zhang, X. W. Li, W. Yang, and G. R. Jin, Quantum Fisher information of entangled coherent states in the presence of photon loss, *Phys. Rev. A* **88**, 043832 (2013).
- [S12] J.-C. Besse, S. Gasparinetti, M. C. Collodo, T. Walter, P. Kurpiers, M. Pechal, C. Eichler, and A. Wallraff, Single-shot quantum nondemolition detection of individual itinerant microwave photons, *Phys. Rev. X* **8**, 021003 (2018).
- [S13] S. Kono, K. Koshino, Y. Tabuchi, A. Noguchi, and Y. Nakamura, Quantum non-demolition detection of an itinerant microwave photon, *Nat. Phys.* **14**, 546 (2018).
- [S14] B. Hacker, S. Welte, S. Daiss, A. Shaikat, S. Ritter, L. Li, and G. Rempe, Deterministic creation of entangled atom-light Schrödinger-cat states, *Nat. Photon.* **13**, 110 (2019).
- [S15] J.-C. Besse, S. Gasparinetti, M. C. Collodo, T. Walter, A. Remm, J. Krause, C. Eichler, and A. Wallraff, Parity detection of propagating microwave fields, *Phys. Rev. X* **10**, 011046 (2020).
- [S16] A. Dragan and K. Banaszek, Homodyne Bell's inequalities for entangled mesoscopic superpositions, *Phys. Rev. A* **63**, 062102 (2001).
- [S17] T. Yu and J. H. Eberly, Evolution from entanglement to decoherence of bipartite mixed “X” states, arXiv preprint quant-ph/0503089 (2005).
- [S18] T. Yu and J. H. Eberly, Quantum open system theory: bipartite aspects, *Phys. Rev. Lett.* **97**, 140403 (2006).
- [S19] S. A. Hill and W. K. Wootters, Entanglement of a pair of quantum bits, *Phys. Rev. Lett.* **78**, 5022 (1997).
- [S20] W. K. Wootters, Entanglement of formation of an arbitrary state of two qubits, *Phys. Rev. Lett.* **80**, 2245 (1998).
- [S21] W. K. Wootters, Entanglement of formation and concurrence., *Quantum Inf. Comput.* **1**, 27 (2001).